PHYSICAL REVIEW B **68**, 241307(R) (2003)

Ultrafast polarization dynamics in biased quantum wells under strong femtosecond optical excitation

D. Turchinovich and P. Uhd Jepsen
Department of Molecular and Optical Physics, Physikalisches Institut, Universität Freiburg, Hermann-Herder-Strasse 3, 79104 Freiburg, Germany

B. S. Monozon
Department of Physics, State Marine Technical University, Lotsmanskaya 3, 190008 St. Petersburg, Russia

M. Koch
Institut für Hochfrequenztechnik, Technische Universität Braunschweig, Schleinitzstrasse 22, 38106 Braunschweig, Germany

S. Lahmann, U. Rossow, and A. Hangleiter
Institut für Technische Physik, Technische Universität Braunschweig, Mendelssohnstrasse 2, 38106 Braunschweig, Germany
(Received 1 August 2003; revised manuscript received 16 September 2003; published 22 December 2003)

We observe ultrafast polarization dynamics in strongly internally biased InGaN/GaN multiple quantum wells during intense femtosecond optical excitation. In the case of strong enough excitation we demonstrate that the built-in bias field (on the order of MV/cm) can be completely screened by the carriers excited in spatially separated states. The removal of the initial strong bias leads to dynamical modification of the band structure, the electron and hole wave functions, and the absorption coefficient within the duration of the excitation pulse. We show that such an optically induced dynamical screening of the biased quantum well can be described in terms of discharging of a nanoscale capacitor driven by a femtosecond laser pulse. The electrostatic energy stored in the capacitor is released via THz emission. Due to its nonlinearity such a process may lead to emission of a THz pulse with bandwidth significantly exceeding that of the excitation pulse.

DOI: 10.1103/PhysRevB.68.241307 PACS number(s): 73.63.Hs, 72.20.Ht, 78.67.De

In recent years a variety of methods have been developed to generate broadband THz pulses with femtosecond laser pulses. Time- and field-resolved detection of such THz pulses has been used to investigate various physical mechanisms which give rise to THz emission.[1–4]

Here we describe the polarization dynamics in a quantum-sized structure in a strong electric field of several MV/cm, driven by intense femtosecond (fs) excitation with fluences of the order of mJ/cm^2. The choice of this regime generalizes results from earlier studies of polarization dynamics in externally biased quantum wells (QW's) under weak fs excitation, where effects caused by the electric field created by excited carriers were negligible,[1] and studies of carrier dynamics in strongly biased *p-i-n* structures, where quantum confinement played no role due to the large dimensions of the devices.[4]

In a biased QW the electron-hole pairs are created in polarized states. The electric field of such an optically created dipole has a polarity opposite to that of the bias field. This leads to a partial screening of the initial bias field, and therefore to partial removal of the initial bias. At strong and fast enough excitation it is possible to screen the bias field completely since enough polarized electron-hole pairs can be created in a time interval much shorter than their typical recombination time. Driven by a fs laser pulse, the excitation of polarized electron-hole pairs and the screening of the initial bias field results in an ultrafast polarization change within the excitation pulse duration, leading to THz emission (see, e.g., Ref. 1).

Screening of a biased QW driven by a short laser pulse is a strongly nonlinear process. Once the first photons of the leading edge of the excitation pulse are absorbed the bias field is partially screened. Consequently, the overlap of the electron and hole wave functions and therefore also the absorption coefficient increase for the next photons to come. Hence, the absorption coefficient and therefore the resulting partial screening of the QW will at any time depend completely on the screening action of all photons that were absorbed previously.

To study the above effects we have chosen low-pressure metalorganic vapor phase epitaxy grown InGaN/GaN QW's for their large built-in electric fields. Our samples consist of ten identical $In_{0.2}Ga_{0.8}N$ QW's separated by 7.2-nm GaN barriers, and a 2-μm-thick near-intrinsic GaN buffer layer. We studied two different samples with QW widths L_z of 2.7 and 3.6 nm, respectively, with a built-in field strength of 3.1 MV/cm, directed against the growth direction.[5,6] The electric fields in the inner and outer barriers are weaker, and have a polarity opposite to the field inside the QW's.

We use the frequency doubled output from a Ti:sapphire-based regenerative amplifier system (Clark MXR, CPA 1000) with photon energy of 3.1 eV (400 nm wavelength), a pulse duration of 120 fs, a repetition rate 1 kHz, and a fluence of up to 1.3 mJ/cm^2. The laser beam spot area at the sample is about 3×1.5 mm^2. The photon energy of 3.1 eV is enough to excite electron-hole pairs in our QW's both in the biased and in the completely screened cases [see Fig. 1(a)], but not in the barriers. The emitted THz pulses are detected by free-space electro-optic sampling in a 1-mm-thick ZnTe crystal.[7] The detector bandwidth is restricted to the range 0.1–3 THz due to THz absorption and phase-mismatch effects.[8]

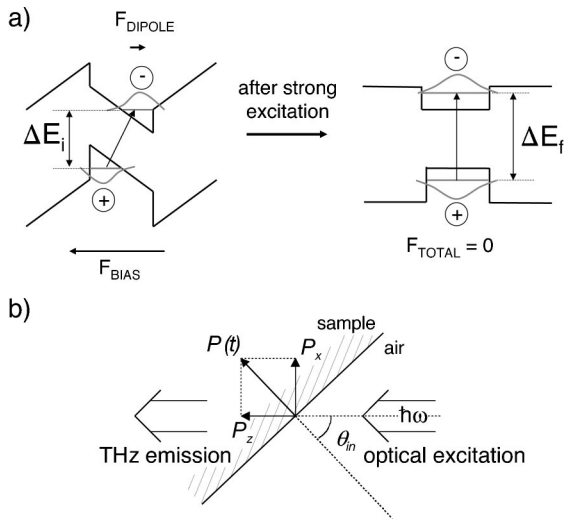

FIG. 1. (a) Excitation of polarized and unpolarized electron-hole pairs in biased and screened QW, respectively. (b) Sample and polarization geometry. $P(t)$—transient polarization, P_x and P_z are its components perpendicular and parallel to the THz propagation axis, respectively.

Simultaneously with the THz pulse detection we measure the time-integrated photoluminescence (PL) spectra from our samples using a fiber-coupled spectrometer (Ocean Optics S2000). All the measurements are performed at room temperature.

Our excitation geometry is illustrated in Fig. 1(b). The built-in field is perpendicular to the sample surface. To obtain a nonzero projection P_x of the transient dipole vector in the direction orthogonal to the propagation direction of the THz pulse we tilt the sample to an angle θ_{in} of 45°. Figure 2(a) shows THz pulses generated in the sample with $L_z = 2.7$ nm with an excitation fluence ranging from 0.02 to 1.3 mJ/cm^2. The shape of the THz pulses is identical for all excitation intensities and is determined by the limited bandwidth of our setup. Since the detected pulse shape remains unchanged at all excitation fluences, the square of the peak field strength is proportional to the total pulse energy.

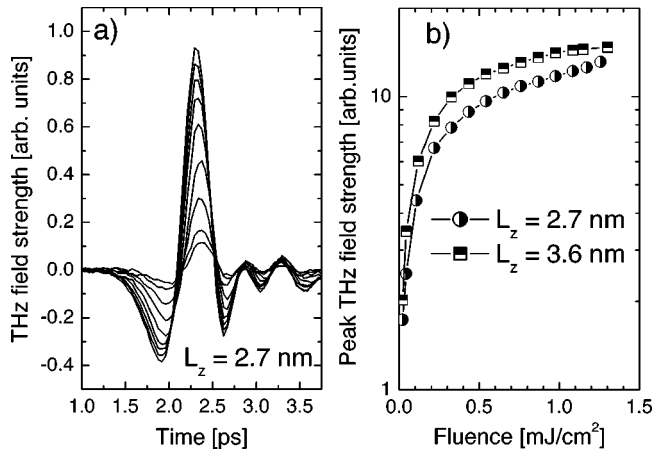

FIG. 2. (a) THz pulses detected from a sample with $L_z = 2.7$ nm at excitation fluences 0.02, 0.04, 0.11, 0.22, 0.43, 0.65, 0.87, 1.09, and 1.26 mJ/cm^2. (b) Dependency of peak-peak electric-field strength of THz pulses on excitation fluence for the samples with $L_z = 2.7$ and 3.6 nm.

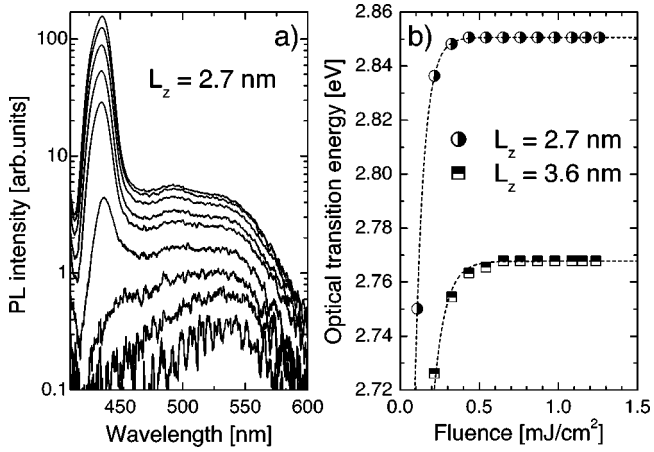

FIG. 3. (a) Time-integrated PL spectra detected from a sample with $L_z = 2.7$ nm at excitation fluences 0.02, 0.04, 0.11, 0.22, 0.43, 0.65, 0.87, 1.09, and 1.26 mJ/cm^2. (b) Dependency of PL maximum on excitation fluence for the samples with $L_z = 2.7$ and 3.6 nm. Lines are guides to the eye.

In Fig. 2(b) the dependency of the peak-peak amplitudes on the excitation fluence for the pulses generated in the two samples is shown. Initially the pulse amplitudes grow rapidly with the optical intensity. This initial rise is followed by a saturation for fluences higher than 0.5 mJ/cm^2. The sample with wider QW's produces stronger pulses. When θ_{in} is reversed to $-45°$, thereby reversing the sign of P_x, the THz pulses also change their polarity. When the samples are excited at normal incidence no THz emission is detected. Both these observations show that the THz emission is related exclusively to the built-in bias field directed perpendicular to the sample surface.

In Fig. 3(a) the time-integrated PL spectra for the sample with $L_z = 2.7$ nm at excitation fluences in the range 0.02–1.3 mJ/cm^2 are shown. At weak excitation a broad line is observed with its maximum at a wavelength of 540 nm. With increasing excitation fluence we observe a broadening of this line to shorter wavelengths as well as a growth in amplitude. Above a certain excitation fluence a strong and narrow blue-shifted line appears. This line moves to 435 nm and remains at this spectral position with further increase in excitation fluence. We attribute the PL at weak excitation to recombination in the biased QW both because of its spectral position and its weak intensity. The blue-shifted line appearing at higher fluences is attributed to recombination in the partially or completely screened QW. The fact that the PL peak does not shift to shorter wavelength than 435 nm with further increase in excitation fluence indicates that complete screening of the QW is reached within our excitation fluence range. The PL spectrum at strong excitation fluence is a superposition of optical transitions in a continuous range of electric fields from zero, when the QW is screened to its maximum value of 3.1 MV/cm, when all the carriers have recombined. The spectral positions of transitions in both the

completely screened and completely biased QW are in agreement with band-structure simulations.[6] The spectral position of the blue-shifted line as function of excitation fluence for the two samples is shown in Fig. 3(b). This blue shift was also observed in similar samples with increase in excitation fluence in the cw regime.[9]

The results of both THz and PL measurements lead us to the conclusion that the polarization dynamics in our samples is related to the dynamical removal of the bias by the excited polarized electron-hole pairs.

The saturation of the THz pulse amplitude with increasing excitation fluence can be understood intuitively if we consider the QW structure as a nanoscale capacitor.

Although the energy released with the THz pulse ultimately originates from the incoming laser pulse,[10] the energy transfer from the excitation pulse to the THz pulse is mediated by the partial or complete discharge of the nanocapacitor. Therefore the maximum THz pulse energy is limited by the electrostatic energy stored in the nanocapacitor.

The energy in the capacitor is $U=\frac{1}{2}\epsilon\epsilon_0 A d F^2$, where $\epsilon\epsilon_0$ is the static permittivity, A is the area, d is the effective width of the capacitor, and F is the electric field inside the capacitor. The stored energy is hence directly proportional to the width d, determined by the initial displacement of the electron and hole wave functions (rather than simply the QW width). The initial distance between the mean weighted maxima of the electron and hole wave functions for the wider well is larger than for the narrow one, and thus more electrostatic energy is stored in the wider well. For our sample with $L_z=3.6$ nm we estimate the stored electrostatic energy density to be $\approx 0.5\ \mu\mathrm{J/cm}^2$. This is consistent with the total energy of the strongest THz pulse detected in our experiments. According to the nanoscale capacitor model the THz pulse energy (and therefore electric-field amplitude) should saturate as the total stored electrostatic energy is released. Experimentally we do not observe a full saturation behavior, most probably due to the Gaussian profile of the excitation beam which will always leave underscreened areas at the edges of the excitation spot given the large dimensions of the excitation spot

The screening of the biased QW with a laser pulse is expected to be a strongly nonlinear process. We performed a simulation of the wave-function and band-structure dynamics in our samples, subject to intense fs excitation. We applied an infinite QW variational approach by Bastard *et al.*[11] in order to provide the continuity of results in strong, medium, weak, and zero electric-field regimes. In order to account for finite barriers we introduced modified effective masses.[12] Relevant material parameters were taken from the literature.[9,13,14] Our simulations only consider the ground states for electrons and holes in the QW. Taking the excited states into account will not change the results qualitatively. The details of our theoretical approach will be published elsewhere.[15]

In Fig. 4(a) the dynamics of the ''empty'' wave functions, i.e., the wave functions representing states to be filled by the carriers created by the next excitation photons, is shown for the sample with $L_z=2.7$ nm. For excitation we assume a 120 fs pulse with a wavelength of 400 nm and a fluence of

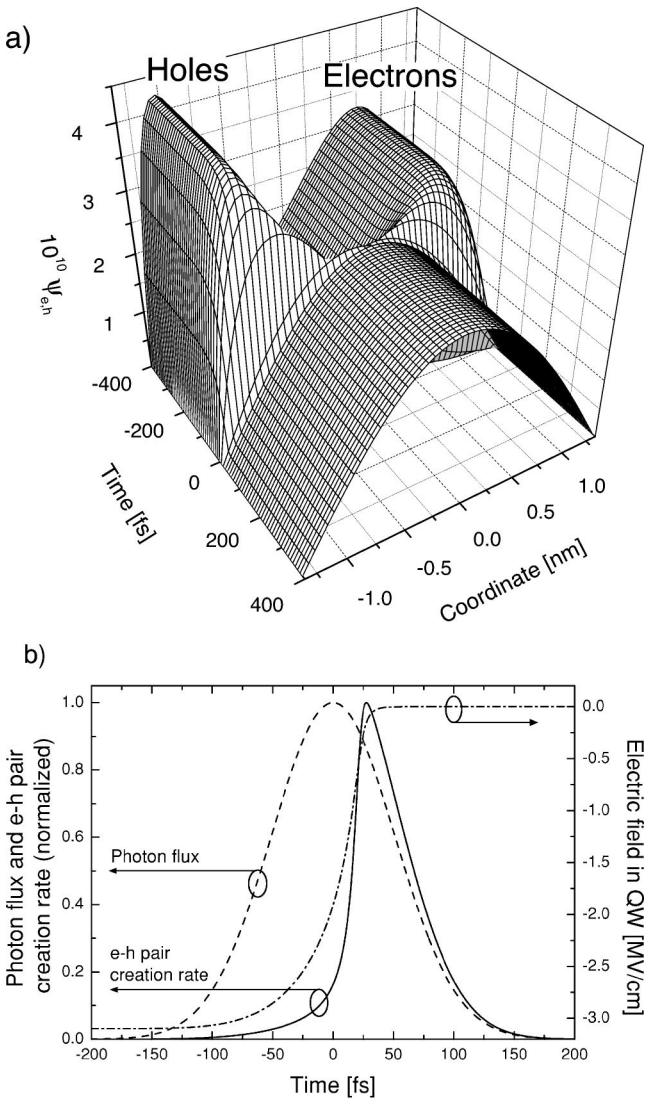

FIG. 4. (a) Temporal evolution of the ''empty'' wave functions $\psi_{e,h}$ for electrons and holes during the strong pulsed excitation. (b) Evolution of incident photon flux (dashed line), resulting electric field in the QW (dash-dotted line), and electron-hole pair-creation rate (solid line) during the strong pulsed excitation.

$0.7\ \mathrm{mJ/cm}^2$. At negative times the wave functions are strongly separated as a result of the strong initial bias. The displacement of the hole wave function is larger than that of the electron wave function due to the larger effective mass of the hole. As the time approaches zero, the wave functions move towards the middle of the QW, as a result of screening of the built-in field by the previously created carriers. At positive times the ''empty'' wave functions are located at the middle of the QW since the bias has been removed. The electron-hole pairs are excited in nonpolarized states and the nanocapacitor is discharged. Subsequent recharging of the nanocapacitor is completed when all electron-hole pairs in the QW have recombined, and the original bias field is restored.

In Fig. 4(b) the temporal evolution of the electric field in the QW and the electron-hole pair-creation rate is shown together with the excitation pulse profile. Absorption in a

biased QW can be approximated as $\alpha(t)=\alpha_{max}M^2(t)$, where α_{max} is the absorption coefficient of bulk material at comparable excitation conditions and $M(t)$ is the time-dependent overlap integral of the electron and hole wave functions. Thus the absorption coefficient is a dynamical parameter, which depends on the band structure of the sample at each given moment in time. In a biased QW the overlap between the electron and hole wave functions is small, and therefore the absorption is weak. As the QW is screened, the absorption coefficient increases. The maximum of the electron-hole pair-creation rate will always be at $t\geqslant 0$ since the product of the absorption coefficient and the laser intensity always finds its maximum at $t\geqslant 0$. This nonlinear absorption can lead to the total screening of the QW within a fraction of the excitation pulse duration. This leads to the interesting prediction that the bandwidth of the emitted THz pulse may significantly exceed that of the excitation pulse. However, using identical laser pulses for both generation of the THz pulses and subsequent sampling of their temporal shape will not allow experimental verification of this effect. An experiment tailored to detect the high bandwidth based on a long excitation pulse and a short sampling pulse will allow us to verify this effect.

D.T. and P.U.J. acknowledge stimulating discussions with Hanspeter Helm and financial support from DFG (Grant No. SFB 276 TP C14).

[1] P.C.M. Planken, M.C. Nuss, W.H. Knox, D.A.B. Miller, and K.W. Goossen, Appl. Phys. Lett. **61**, 2009 (1992).
[2] H.G. Roskos, M.C. Nuss, J. Shah, K. Leo, D.A.B. Miller, A.M. Fox, S. Schmitt-Rink, and K. Köhler, Phys. Rev. Lett. **68**, 2216 (1992).
[3] Y. Hokomoto, Y. Kadoya, and M. Yamanishi, Appl. Phys. Lett. **74**, 3839 (1999).
[4] A. Leitenstorfer, S. Hunsche, J. Shah, M.C. Nuss, and W.H. Knox, Phys. Rev. Lett. **82**, 5140 (1999).
[5] J.S. Im, H. Kollmer, J. Off, F. Scholz, and A. Hangleiter, Mater. Sci. Eng., B **59**, 315 (1999).
[6] A. Hangleiter, F. Hitzel, S. Lahmann, and U. Rossow, Appl. Phys. Lett. **83**, 1169 (2003).
[7] Q. Wu and X.-C. Zhang, Appl. Phys. Lett. **68**, 1604 (1996).
[8] M. Schall and P. Uhd Jepsen, Appl. Phys. Lett. **77**, 2801 (2000).
[9] T. Takeuchi, S. Sota, M. Katsuragawa, M. Komori, H. Takeuchi, H. Amano, and I. Akasaki, Jpn. J. Appl. Phys., Part 2 **36**, L382 (1997).
[10] A. Shimizu and M. Yamanishi, Phys. Rev. Lett. **72**, 3343 (1994).
[11] G. Bastard, E.E. Mendez, L.L. Chang, and L. Esaki, Phys. Rev. B **28**, 3241 (1983).
[12] C. Giner and J. Gondar, Physica B **138**, 287 (1986).
[13] J. Wagner, H. Obloh, M. Kunzer, M. Maier, K. Köhler, and B. Johs, J. Appl. Phys. **76**, 291 (2000).
[14] J.S. Im, A. Moritz, F. Steuber, V. Härle, F. Scholz, and A. Hangleiter, Appl. Phys. Lett. **70**, 631 (1997).
[15] D. Turchinovich and B. S. Monozon (unpublished).